Macromolecules 1983, *16*, 1115–1120

A Theory of Healing at a Polymer–Polymer Interface

Young Hwa Kim[‡] **and Richard P. Wool***

Materials Research Laboratory and the Department of Metallurgy and Mining Engineering, University of Illinois, Urbana, Illinois 61801. *Received June 1, 1982*

ABSTRACT: Crack healing in polymers has several stages, namely, surface rearrangement, surface approach, wetting, diffusion, and randomization. We present a microscopic theory of the diffusion and randomization stages based on the reptation model of chain dynamics by de Gennes. The theory analyzes motion of chains at the interface and calculates the average interpenetration distance χ of polymer segments as a function of time t and molecular weight M. The theory predicts that, when fracture stress σ is proportional to χ, (i) $\sigma/\sigma_\infty \sim t^{1/4}M^{-3/4}$ for $t < T_r$, where T_r is the tube renewal time of the reptation model and σ_∞ is the virgin fracture stress, and (ii) the $t^{1/4}$ dependence persists for a wide range of M and also for time t until t becomes comparable to T_r. These results are in agreement with healing experiments.

1. Introduction

Crack healing in polymeric materials has been the subject of active investigations in recent years.[1-6] When two similar pieces of bulk polymer are brought into good contact at a temperature above the glass transition, the interface gradually disappears and mechanical strength at the polymer–polymer interface develops as the crack heals. This crack healing is primarily due to the diffusion of chains across the interface. The chain diffusion across the interface is a special type of mass transfer, which cannot be described by the conventional diffusion equation. The study of crack healing in polymers is important for the understanding of the mechanical strength at a polymer–polymer interface at the level of chain dynamics because it is related to various polymer engineering problems such as polymer–polymer welding and the preparation of a bulk thermoplastic from small resin particles. Recently, Wool and O'Connor[6] studied crack healing in terms of the following stages: (i) surface rearrangement, (ii) surface approach, (iii) wetting, (iv) diffusion, and (v) randomization. By the end of the wetting stage, potential barriers associated with the inhomogeneities at the interface disappear and chains are free to move across the interface in the following stages of diffusion and randomization. The latter stages of diffusion and randomization are the most important ones because the characteristic strength of a polymer material appears in these stages. The essential features of chain motions in a bulk material consisting of entangled random coil chains are properly described by the reptation model, which was developed by de Gennes[7] and later by Doi and Edwards.[8] The model has been applied to the problem of crack healing at the polymer–polymer interface by de Gennes,[3] Prager and Tirrell,[5] and Wool and O'Connor.[6] In the crack healing problem, there is a basic question to be answered. The question is "How does one relate the microscopic description of motion of chains to the macroscopic measurements such as fracture stress?" Also, the initial conformations of chains and even the applicability of the reptation model in the case of highly oriented initial conformation of chains on the surfaces of melts should be considered. There are no exact answers to these questions yet. Therefore, one has to make a number of assumptions in order to apply the reptation model to the crack healing problem. The purpose of this paper is to present an application of the reptation model to the crack healing problem with assumptions and points of view different from those in the previous works.[3,5] In section 2, the reptation model is briefly reviewed. Then the concept of minor chains is introduced, which plays the central role in this paper. In section 3, chain motions at the interface are investigated with the help of the concept of minor chains. Here, quantitative analysis of chain motions is performed. In section 4, mechanical measurement such as fracture stress is related to chain motions at the interface. Conclusions and discussion are made in the last section.

2. Chain Motions in Amorphous Polymeric Materials

In a bulk amorphous polymeric material, the motion of a chain is greatly restricted by the entangelements of neighboring chains. The reptation model is suitable to describe the motion of a chain that is entangled with many other chains. According to the reptation model, the constraints imposed on a chain by the entanglements of chains effectively confine a chain inside a tube-like region.[8,9] Due to thermal fluctuations, a chain is conceived as wriggling around in the tube. de Gennes[7] argued that the wriggling motions occur rapidly, that their magnitudes are small, and that in a time scale greater than that of the wriggling motions, a chain, on average, moves coherently back and forth along the center line of the tube with a certain diffusion constant, keeping its arc length constant. Therefore, a chain as a whole executes a one-dimensional random motion along the tube. The chain conformation at a given moment is the same as the shape of the tube that confines the chain at the same moment. For a chain to change its conformation, it has to disengage itself from the tube that was defined at an earlier moment. When a chain moves "forward", the "head" of the chain chooses its direction randomly and when it moves "backward", the "tail" chooses its direction randomly. In order to see how a chain disengages itself from the initial tube, chain conformations at different times are shown in Figure 1. In Figure 1, the tube defined at time $t = 0$ (i.e., the initial tube) is shown as two dotted lines at various times. At $t = t_1$, some end portions of the chain have already "escaped" from the initial tube. The portions of a chain that are no longer in the initial tube increase with time and will be referred to as minor chains. The random coil spherical envelopes enclosing the minor chain at different times are shown in circles. A minor chain has length $l(t)$, which is an increasing function of time t, and it has the conformation of a random Gaussian chain. The minor chains are the portions of chains that have lost the memory of the initial conformations of chains. As the minor chains become longer, the initial conformations are gradually replaced by new conformations.

There are two basic time scales in the reptation model, namely, T_e and T_r. The first one, T_e, is the time associated with short-range wriggling motions of a chain in the tube; T_r is the amount of time taken for a chain to disengage

---

[‡] Present address: Central Research Laboratory, 208-1, 3M Center, St. Paul, MN 55144.

0024-9297/83/2216-1115$01.50/0 © 1983 American Chemical Society

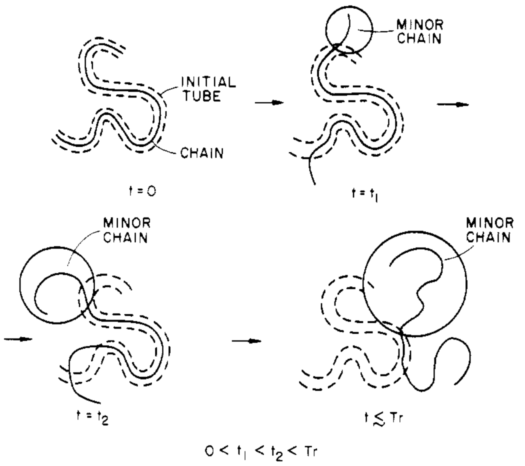

Figure 1. Disengagement of a chain from its initial tube. The emergence and growth of minor chains are also shown. T_r is the tube renewal time.

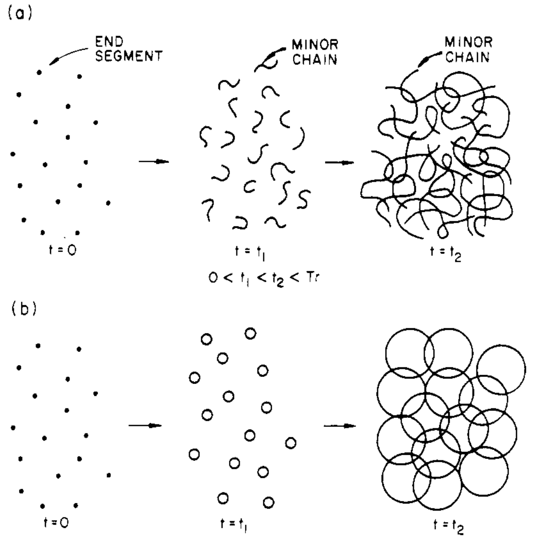

Figure 2. (a) Minor chains at different times $t < T_r$. (b) Increasing spherical envelopes of minor chains at different times.

itself completely from the initial tube (T_r is called the tube renewal time). de Gennes[7] showed that $T_e \propto M^2$ and $T_r \propto M^3$, where M is the molecular weight of the linear chains. Since M is typically large, T_e is much smaller than T_r. The time scale of importance in a crack healing problem is in the region of $T_e < t < T_r$. Therefore, T_e will be ignored from now on, with the understanding that t is always greater than T_e when $t > 0$. In Figure 2a, the minor chains at different times are shown. At $t = 0$, only the locations of the end segments are shown because the minor chains start to grow at the end segments. The increase in length of the minor chains is shown at times t_1 and t_2 in Figure 2a. In Figure 2b, the average shape and size of the ensemble of minor chains that can emerge from a given initial distribution of end segments are shown at different times. The locations of the end segments at $t = 0$ and the increasing spherical envelopes of minor chains at t_1 and t_2 are shown in Figure 2b. The concept of minor chains turns out to be very useful when chain motions at the interface are studied in the next section.

3. Chain Motions at a Polymer–Polymer Interface

3.1. Characterization of Chain Motions at the Interface. The conformation of two chains at the interface before and after the stages of diffusion and randomization are shown in Figure 3. At $t = 0$, the chains are separated by the interface. However, at $t \gtrsim T_r$, the chains cross the interface, interpenetrate into the other side, and make entanglements with chains of the other side. Let us consider the motion of a chain at the interface from the point of view of the reptation model. The conformations of a chain at the interface are shown at different times in Figure 4. At $t = 0$, a chain and its initial tube at the interface are shown. At $t = t_1$, the minor chains that have "escaped" from the initial tube are shown. The minor chains may assume any conformation of random chains and they may also cross the interface. Only the portions of the initial tube that still confines part of the chain are shown. At a later time of $t = t_2$, the minor chains are much longer. They may cross the interface many times and penetrate into the other side more deeply. Small portions of the chain are still confined in the initial tube.

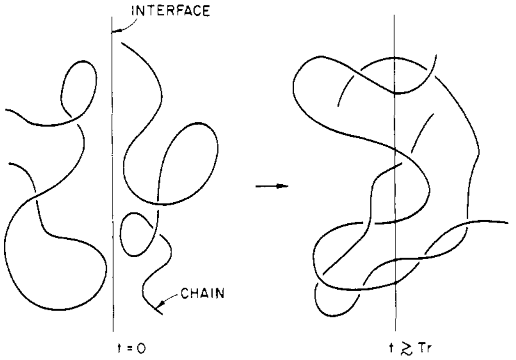

Figure 3. Conformations of two chains at the interface before and after the stages of diffusion and randomization.

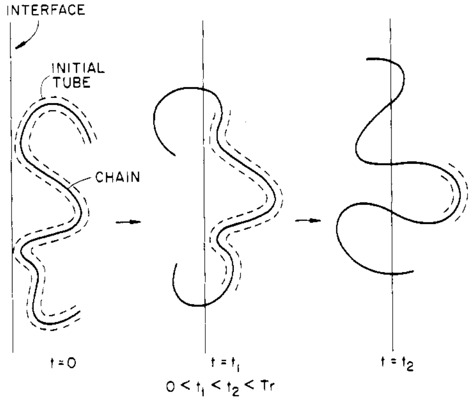

Figure 4. Disengagement of a chain from its initial tube near the interface. Only portions of the initial tube that still confines part of the chain are shown.

Now let us consider the minor chains at the interface. It can be shown that the distribution of end segments is uniform when the chain conformations are equilibrated with the surface (i.e., before the stages of diffusion and randomization), and we assume that this is the case in this paper. In Figure 5a, the minor chains that emerged from one side of the interface (vertical lines) are shown at different times. It is important to notice that only minor chains may cross the interface. Therefore, Figure 5a shows the portions of chains that are responsible for the mass transfer of chain segments across the interface. At $t = 0$, chain conformations at or near the interface are not in equilibrium and chains are now free to cross the interface while they are still separated into two groups. Then the minor chains emerge and grow out of the initial nonequilibrium conformations. The minor chains do not encounter any obstacles at the interface and they assume spherically symmetric Gaussian conformations as they interpenetrate across the interface (Figure 5b). The growth and random Gaussian conformations of the minor chains

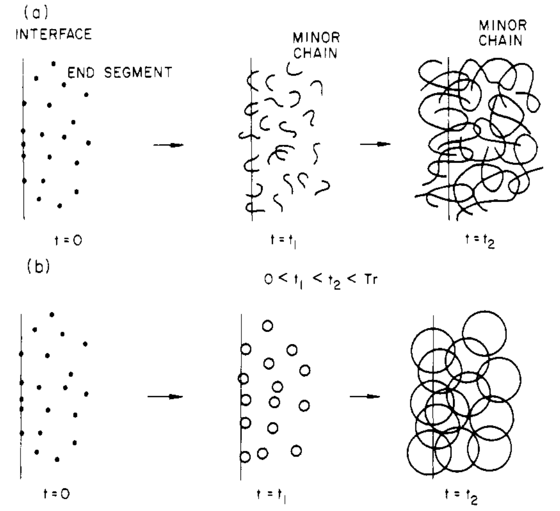

Figure 5. (a) Motion of minor chains that have emerged from one side of the interface. (b) Growth of the spherical envelopes of minor chains that have emerged from one side of the interface.

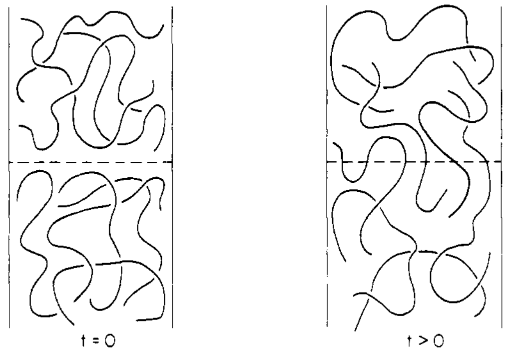

Figure 6. Conventional point of view of chain motions across the interface.

constitute the diffusion and randomization of chains across the interface. This point of view of motion of chains at the interface may be compared with a more conventional point of view,[1,3,5] which is shown in Figure 6. Figure 6 is the picture one would imagine if one tries to keep track of motions of entire chains at the interface. Figure 5a, instead, shows only those portions of chains (i.e., minor chains) that contribute to the mass transfer across the interface. The behavior of minor chains is easy to understand once the length of a minor chain, $l(t)$, is obtained as a function of time, t, and other parameters such as molecular weight, M, because the conformations of the minor chains are always Gaussian in the bulk and at the interface as well. Let us consider a chain near the interface. Let ξ be the distance of an end segment from the interface. At $t = 0$, the conformation of a chain with two end segments at $\xi = \xi_1$ and $\xi = \xi_2$ is determined by the partition function $Z(\xi_1,\xi_2)$ as

$$Z(\xi_1,\xi_2) = (\gamma/\pi)^{1/2}[\exp\{-\gamma(\xi_1 + \xi_2)^2\} + \exp\{-\gamma(\xi_1 - \xi_2)\}^2] \tag{1}$$

where $\gamma = 1/2a^2N$, a is the length of one segment, and N is the number of segments of a chain. However, at $t \gtrsim T_r$, the equilibrium conformation is determined by $Z_e(\xi_1,\xi_2)$, where

$$Z_e(\xi_1,\xi_2) = (\gamma/\pi)^{1/2} \exp\{-\gamma(\xi_1 - \xi_2)^2\} \tag{2}$$

which is Gaussian.

The stages of diffusion and randomization are characterized by the transition of chain conformations from $Z(\xi_1,\xi_2)$ to $Z_e(\xi_1,\xi_2)$. This transition is shown in Figure 7.

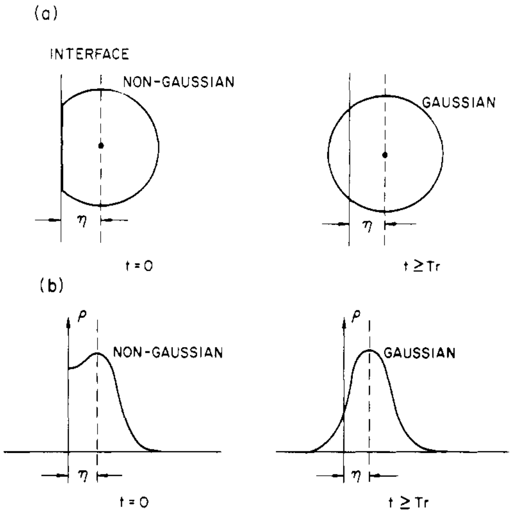

Figure 7. (a) Average shape and size of a chain at the interface before and after healing. (b) Segment density, ρ, of the chain in (a) before and after healing.

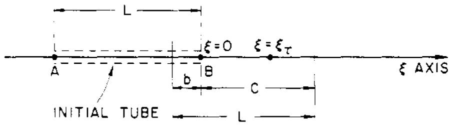

Figure 8. Coordinate of the one-dimensional random walk of a chain in its tube for the derivation of $\langle l \rangle$.

In Figure 7a, the average shape and size of a chain at the interface (solid vertical line) before and after the transition are shown. The distance η from the location of the highest segment density of that chain to the interface is shown to be constant throughout the transition. In Figure 7b, the segment density, ρ, of that chain before and after the transition is shown. This transition is accomplished by the time behavior of the minor chains. The time for this transition to occur is the tube renewal time, T_r. Therefore, the stages of diffusion and randomization are finished by the time $t \approx T_r$. Even for $t > T_r$, chains of spherically symmetric, Gaussian conformations diffuse across the interface. However, this type of chain diffusion is irrelevant to the crack healing problem of identical polymer chains. When $t < T_r$, the conformation of a chain near the interface cannot be a Gaussian one because the overall segment density of the polymer material is maintained constant throughout the crack healing stages. Therefore, the stages of diffusion and randomization are characterized by the relaxation of conformation of chains from the non-Gaussian to the Gaussian one. During the transition, formation of links (or bridges) between the two blocks and new entanglements between the two groups of chains are all accomplished by the motions and growth of the minor chains.

3.2. Analysis of Chain Motions at the Interface. In order to derive $l(t)$, let us consider the one-dimensional random walk of a chain in its tube as shown in Figure 8. The ξ axis is the curvilinear distance a chain travels and the tube is shown as two dotted lines. At $t = 0$, end segments A and B are located at $\xi = -L$ and $\xi = 0$, respectively. The location of B after τ steps of random walk is denoted by ξ_τ. There are two distances, b and c, to be considered, where $b + c = L$ is required. In this paper, we derive $\langle l \rangle$, the average of $l(t)$. Let $G(b,c,\xi_\tau)$ be the fraction of the number of walks of τ steps from $\xi = 0$ to $\xi = \xi_\tau$, with two absorbing walls at $\xi = -b$ and $\xi = c$. The end segment B is not allowed to "touch" the absorbing walls. This is given by

$$G(b,c,\xi_\tau) = (\beta/\pi)^{1/2}\sum_{m=0}^{\infty}[\exp(-\beta\{2m(b+c)+\xi\}^2) + \exp(-\beta\{2m(b+c)-\xi^2\}) - \exp(-\beta\{2m(b+c)+2b+\xi\}^2) - \exp(-\beta\{2m(b+c)+2c-\xi\}^2)] - (\beta/\pi)^{1/2}\exp(-\beta\xi^2) \tag{3}$$

where $\beta = 1/2a^2\tau$ and a is the length of one step. The length a depends on the overall segment density of a system but it does not depend on the molecular weight.[8] For the derivation of $\langle l\rangle$, it is necessary to obtain $J(b,c,\xi_\tau)$, which is the fraction of the number of random walks of τ steps from $\xi = 0$ to $\xi = \xi_\tau$ for $-b \le \xi_\tau < c$ with at least one "touch" at $\xi \equiv -b$ where $b + c = L$. This is because when the end segment B arrives at $\xi = -b$, the part of the initial tube from $\xi = -b$ to $\xi = 0$ is destroyed. The length of the minor chain of end segment B is $b + \xi_\tau$. The same rule applies to the end segment A. This is related to $G(b,c,\xi_\tau)$ as follows:

$$J(b,c,\xi_\tau) = a\frac{\partial}{\partial b}G(b,c,\xi_\tau) \tag{4}$$

The average of l, that is, $\langle l\rangle$, is equal to $\langle b\rangle$ due to the symmetry of the chain motion with respect to the "head" and "tail" of the chain. Therefore, we have

$$\langle l\rangle = \int_0^L \mathrm{d}b\; b\int_{-b}^{L-b}\mathrm{d}\xi_\tau\; J(b,L-b,\xi_\tau)\Big/\int_{-b}^{L-b}\mathrm{d}\xi_\tau\; J(b,L-b,\xi_\tau) \tag{5}$$

From (3), (4), and (5), $\langle l\rangle$ is given by

$$\langle l\rangle = k_2(x)/k_1(x) \tag{6}$$

where

$$k_1(x) \equiv a\sum_{m=0}^{\infty}[(6m+2)\,\mathrm{erf}\,(2mx+x) - (6m+1)\,\mathrm{erf}\,(2mx) - (2m+1)\,\mathrm{erf}\,(2mx+2x) + 2m\,\mathrm{erf}\,(2mx-x)] \tag{6a}$$

and

$$k_2(x) \equiv \frac{aL}{\pi^{1/2}x}\sum_{m=0}^{\infty}[\exp\{-(2mx)^2\} - 2\exp\{-(2mx+2x)^2\} + \exp\{-(2mx+2x)^2\}] + aL\sum_{m=0}^{\infty}[(m+1)\,\mathrm{erf}\,(2mx+2x) - (m+1)\,\mathrm{erf}\,(2mx+x) - m\,\mathrm{erf}\,(2mx) + m\,\mathrm{erf}\,(2mx-x)] \tag{6b}$$

where $x \equiv L/(2a^2\tau)^{1/2}$ and erf (x) is the error function of variable x.

The asymptotic form of $\langle l\rangle$ at early times, that is, when $a^2\tau < L^2$, is obtained as follows.

$$\lim_{x\to\infty}[\mathrm{erf}\,(x)] \simeq 1 - \exp(-x^2)/(\pi^{1/2}x) \tag{7}$$

From (6) and (7), we have

$$\langle l\rangle \approx a(2\tau/\pi)^{1/2}(1 - \exp\{-L^2/2a^2\tau\}) \tag{8}$$

when $a^2\tau < L^2$. The conversion from τ to t is given by

$$\tau = 2Dt/a^2 \tag{9}$$

where D is the curvilinear diffusion constant, which is proportional to $1/M$.[7] Therefore, we have

$$\langle l\rangle \approx 2(Dt/\pi)^{1/2}[1 - \exp\{-L^2/2Dt\}] \tag{10a}$$

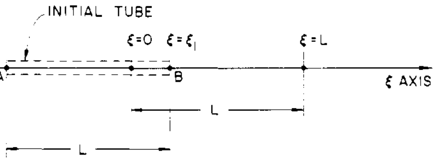

Figure 9. Coordinate of the one-dimensional random walk of a chain in its tube for the derivation of α_t.

From (10a), we find that

$$\langle l\rangle \approx 2(Dt/\pi)^{1/2} \tag{10b}$$

until t becomes comparable to T_r, since $T_\mathrm{r} \approx L^2/(2D)$ and $t < T_\mathrm{r}$. This is an important result. de Gennes derived eq 10b by using scaling arguments,[3] too. It shows that at early times of diffusion and randomization, $\langle l\rangle$ is proportional to $t^{1/2}$. The relation of $\langle l\rangle \propto t^{1/2}$ applies to a wide range of values of M at early times because of the exponential term in (10a). Once $\langle l\rangle$ is obtained, the average interpenetration distance of chains or the number of links (or bridges) and others can be calculated easily. So far, only $\langle l\rangle$, the average of $l(t)$ is calculated. In reality, $l(t)$ has a distribution around $\langle l\rangle$. Also, $\langle l\rangle$ should approach $L/2$ as $t \to \infty$. These aspects are considered now. Let α_t be the fraction of number of chains that have disengaged themselves completely from their initial tubes at time t. In order to derive α_t, let us define $f(\xi_1,L,t)$ as the probability that a one-dimensional random walk that starts at $\xi = \xi_1$ will terminate at $\xi = 0$ for $t > 0$ when there are two absorbing walls at $\xi = 0$ and $\xi = L$ (see Figure 9). In Figure 9, the initial locations of the end segments are denoted as A and B, and the initial tube is shown as two dotted lines. We need to define another quantity $H(\xi_1,L,t)$ as the probability that a one-dimensional random walk that starts at $\xi = \xi_1$ will terminate at $\xi = 0$ or $\xi = L$ at t when there are two absorbing walls at $\xi = 0$ and $\xi = L$. This is given by

$$H(\xi_1,L,t) = f(\xi_1,L,t) + f(L-\xi_1,L,t) \tag{11}$$

Then α_t is given by

$$\alpha_t = \int_0^t \mathrm{d}t\int_0^L \mathrm{d}\xi_1\; H(\xi_1,L,t)\Big/\int_0^\infty \mathrm{d}t\int_0^L \mathrm{d}\xi_1\; H(\xi_1,L,t) = \sum_{\nu=1}^{\infty}\frac{\{1-(-1)^\nu\}}{\nu^2}\left[1 - \exp\left\{-\frac{\pi^2 D\nu^2 t}{L^2}\right\}\right]\Big/\sum_{\nu=1}^{\infty}\frac{\{1-(-1)^\nu\}}{\nu^2} \tag{12}$$

It is obvious that $\alpha_t \to 1$ as $t \to \infty$. From (12), we find that $\alpha_t \approx 0$ until t becomes comparable to T_r due to the exponential term and the factors of $1/\nu^2$ in the numerator. Therefore, for $0 < t < T_\mathrm{r}$, it may be assumed that $\alpha_t = 0$.

Next, let us check if $\langle l\rangle$ approaches $L/2$ as $t \to \infty$. When $t \to \infty$, the following form of $G(b,c,\xi_\tau)$ is more useful to derive $\langle l\rangle$.

$$G(b,c,\xi_\tau) = \frac{2}{b+c}\sum_{m=1}^{\infty}\sin\left(\frac{\pi mb}{b+c}\right)\sin\left(\frac{\pi m(b+\xi)}{b+c}\right)\times\exp\left[-\frac{\pi^2a^2m^2t}{2(b+c)^2}\right] \tag{13}$$

From (13), (4), and (5), $\langle l\rangle$ is given by

$$\langle l\rangle = (L/2)\sum_{m=1}^{\infty}\exp\left[-\frac{\pi^2a^2m^2t}{2L^2}\right]\left[\frac{1-(-1)^m}{m^2}\right]\times\left(\frac{\pi^2a^2m^2t}{L^2}+1\right)\Big/\sum_{m=1}^{\infty}\exp\left[-\frac{\pi^2a^2m^2t}{2L^2}\right]\left[\frac{1-(-1)^m}{m^2}\right]\times\left(\frac{\pi^2a^2m^2t}{L^2}+3\right) \tag{14}$$

From (14), it is clear that $\lim_{t\to\infty}\langle l\rangle = L/2$.

Other quantities such as the average number of links (or bridges) at the interface or the average interpenetration of segments into the opposite side of the interface can also

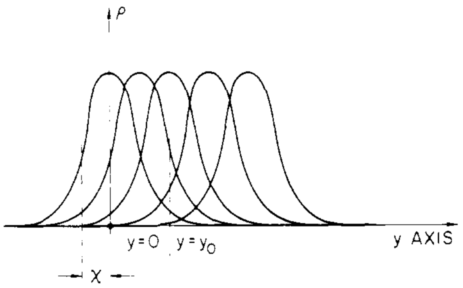

Figure 10. Segment density, ρ, of minor chains and the average interpenetration distance χ.

be calculated through the analysis of the motion of the minor chains at the interface. In this paper, only the average interpenetration distance, χ, of segments is defined and calculated in the next section for the connection between a mechanical measurement and the motion of chains at the interface.

4. Mechanical Measurement

Healing experiments have been conducted on most categories of polymeric materials recently.[6] It is difficult to relate these mechanical measurements to motion of chains at the interface since there is no clear understanding of the connection between these two levels of crack healing phenomena. We shall present our point of view on this problem for fracture stress σ, where σ is equal to the real fracture stress minus the fracture stress due to wetting.[6]

As mentioned in section 3, $l(t)$ has a distribution around $\langle l \rangle$, and the fraction of the number of chains that have disengaged themselves from the initial tube is given by α_t. Let σ be the fracture stress as a function of time t. In general, we may assume that σ has the following form:

$$\sigma = \alpha_t \sigma_L + (1 - \sigma_t) \int_0^L \mathrm{d}l \, P(l) \sigma_l \tag{15}$$

where σ_L is the contribution to σ from a chain that has disengaged itself completely from its initial tube, σ_l is the contribution to σ from a minor chain of length l, and $P(l)$ is the normalized distribution of l. As shown in section 3, α_t is negligible except when t becomes comparable to T_r. Therefore, σ is approximately given by

$$\sigma \approx \int_0^L \mathrm{d}l \, P(l) \sigma_l \tag{16}$$

for $0 < t < T_r$.

Next, we make an assumption that all minor chains have the same length, $\langle l \rangle$. Then σ is given by

$$\sigma \approx \sigma_{\langle l \rangle} \tag{17}$$

This means that for $0 < t < T_r$, σ is mostly due to the minor chains whose average length is equal to $\langle l \rangle$. This is in accordance with our observation in section 3 that only minor chains cross the interface for $0 < t < T_r$. In order to find $\sigma_{\langle l \rangle}$ as a function of $\langle l \rangle$, let us consider the average interpenetration distance, χ, of segments that have crossed the interface. The segment density distribution of a random Gaussian chain is also a Gaussian one. Since the minor chains are uniformly distributed, we have the segment density of minor chains as shown in Figure 10. In Figure 10, y is the coordinate that is perpendicular to the interface (the interface is at $y = 0$), and the segment density, ρ, of individual minor chains that emerged from the region of $y > 0$ is shown as bell-shaped curves. At $t > 0$, some of the segments that belong to these minor chains have already diffused into the region of $y < 0$. The distance χ is the average distance of these segments from the interface. According to this definition, χ is given by

$$\chi = \int_0^\infty \mathrm{d}y_0 \int_0^\infty \mathrm{d}y \, y \times \exp\left[-\frac{(y_0 + y)^2}{2a^2\langle l \rangle}\right] \Bigg/ \int_0^\infty \mathrm{d}y_0 \int_0^\infty \mathrm{d}y \times \exp\left[-\frac{(y_0 + y)^2}{2a^2\langle l \rangle}\right] \tag{18}$$

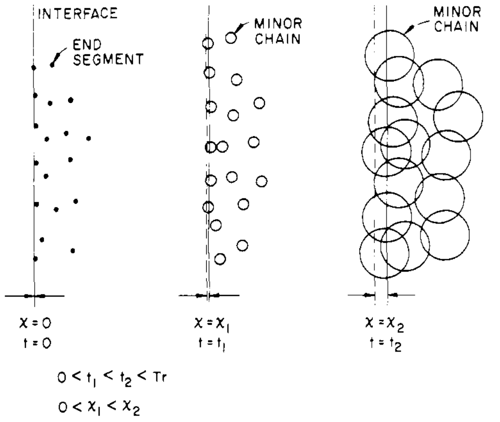

Figure 11. Average interpenetration distance χ and the minor chains of one side of the interface at different times.

From (18), we have

$$\chi \propto \langle l \rangle^{1/2} \tag{19}$$

The distance χ at different times is shown in Figure 11. In order to find the proper form of $\sigma_{\langle l \rangle}$, let us consider σ_∞, which is the fracture stress of a polymeric material of molecular weight M in its virgin state. It is observed experimentally[6,13-15] that for a variety of random coil polymers that

$$\sigma_\infty \propto M^{1/2} \tag{20}$$

for a wide range of M. Also, from (14) and (19) we find that $\chi_\infty \propto M^{1/2}$.

Let us define χ_∞ as the average interpenetration distance of segments of a polymeric material in its virgin state across an imaginary plane. The precise definition of χ_∞ is given by (18), with the replacement of $\langle l \rangle$ with L (the length of a chain). Then we find that

$$\sigma_\infty \propto \chi_\infty \tag{21}$$

Now we assume that

$$\sigma \propto \chi \tag{22}$$

for the following reasons. First, the minor chains are uniformly distributed everywhere and they always have Gaussian conformations. Second, the number of minor chains does not change with time for $0 < t < T_r$. From these aspects and (21), the assumption of (22) is made. Additional reasons for this assumption are found in ref 6. From (10b), (19), (17), and (22), we have

$$\sigma \propto (t/M)^{1/4} \tag{23}$$

for $0 < t < T_r$.

The relation (23) is observed experimentally by Wool and O'Connor.[6] From the analysis of the motion of chains at the interface in section 3, we believe that (23) is valid for a wide range of M and for $0 < t < T_r$ except when t becomes comparable to T_r. When $t \approx T_r$, the stages of diffusion and randomization are essentially completed and the region of $t > T_r$ is of no further interest in this paper. Finally, from (20) and (23) we have

$$\sigma/\sigma_\infty \propto t^{1/4}/M^{3/4} \tag{24}$$

5. Discussion and Conclusions

We have presented a theory of the stages of diffusion and randomization in crack healing of polymeric materials. We studied these stages of crack healing with the following idealizations: (i) All chains have the same length, (ii) up to $t = 0$, chains are not allowed to cross the interface, (iii) at $t = 0$, chains start to diffuse across the interface and all obstacles to the motion of chains across the interface disappear, and (iv) the initial tube of a chain is assumed to be fixed in space. In reality, the tube itself may undergo fluctuations. However, this effect is shown to be negligible for time $0 < t < T_r$.[11,12]

We have the following conclusions:

(i) The stages of diffusion and randomization are characterized by the relaxation of chain conformations from the initial non-Gaussian to the final Gaussian conformation. This relaxation is achieved by the emergence and growth of minor chains.

(ii) The motion of minor chains results in the interpenetration and entanglement of the previously separated group of chains across the interface.

(iii) The fracture stress σ depends on t and M as $\sigma \propto t^{1/4} M^{-1/4}$.

(iv) The $t^{1/4}$ dependence persists for a wide range of M and also for the time t for $0 < t < T_r$ until t becomes comparable to T_r.

Four microscopic models have been suggested to explain the time dependence of mechanical property recovery during healing. (i) Prager and Tirrell[5] assume that the crossing density of molecular contacts or bridges, ρ, is the controlling factor. (ii) de Gennes[3] assumes that the number of bridges, p, across the interface is important. (iii) Jud, Kausch, and Williams[4] assume that the center-of-mass Fickian interdiffusion distance, Y, is important. (iv) We assume that the monomer segment interpenetration distance, χ, is the controlling factor. There is agreement between all groups that the time dependence of the fracture energy, G_{IC}, essentially increases as $G_{IC} \sim t^{1/2}$ and that the fracture stress σ, or the stress intensity factor K_{IC}, behaves as $K_{IC} \sim t^{1/4}$ during healing. However, any model that is used to describe the time dependence of mechanical properties must simultaneously predict both the molecular weight dependence of the healing rate and the molecular weight dependence of the virgin state. Consider the molecular weight dependence of G_{IC} during healing and in the virgin state, $G_{IC}(\infty)$, for each model. (i) Prager and Tirrell's model predicts that $G_{IC} \sim t^{1/2}M^{-3/2}$ and $G_{IC}(\infty) \sim M^0$, i.e., independent of M for all values of M. (ii) de Gennes' model predicts the same results as Prager and Tirrell's model. (iii) Kausch's model predicts that $G_{IC} \sim t^{1/2}M^{-1}$ and $G_{IC}(\infty) \sim M^{1/2}$. (iv) Our model predicts that $G_{IC} \sim t^{1/2} M^{-1/2}$ and $G_{IC}(\infty) \sim M$. Experiments on glassy polymers and uncured elastomers strongly support our model.[13-16]

Acknowledgment. We are grateful for financial support to the Materials Research Laboratory at the University of Illinois, Grant NSF DMR 80-20250, and to the Army Research Office at Durham, NC, Grant DAAG 29-79C-0142.

References and Notes

(1) Voyutskii, S. "Autohesion and Adhesion of Polymers"; Wiley: New York, 1963.
(2) Jud, K.; Kausch, H. *Polym. Bull.* **1979**, *1*, 697.
(3) de Gennes, P.-G. *Hebd. Seances Acad. Sci., Ser. B* **1980**, *291*, 219.
(4) Jud, K.; Kausch, H.; Williams, J. G. *J. Mater. Sci.* **1981**, *16*, 204.
(5) Prager, S.; Tirrell, M. *J. Chem. Phys.* **1981**, *75*, 5194.
(6) Wool, R. P.; O'Connor, K. M. *J. Appl. Phys.* **1981**, *52*, 5953.
(7) de Gennes, P.-G. *J. Chem. Phys.* **1971**, *55*, 572.
(8) Doi, M.; Edwards, S. F. *J. Chem. Soc., Faraday Trans. 2*, **1978**, 1789.
(9) Edwards, S. F. *Proc. Phys. Soc., London* **1967**, *92*, 9.
(10) Yamakawa, H. "Modern Theory of Polymer Solutions"; Harper and Row: New York, 1971.
(11) Klein, J. *Macromolecules* **1978**, *11*, 852.
(12) Daoud, M.; de Gennes, P.-G. *J. Polym. Sci., Polym. Phys. Ed.* **1979**, *17*, 1971.
(13) McCormick, H. W.; Brower, F. M.; Kin, L. *J. Polym. Sci.* **1959**, *39*, 87. For monodisperse PS, the data show that $\sigma_\infty \sim M^{1/2}$ for $M \leq 1.6 \times 10^5$.
(14) Robertson, R. E. In *Adv. Chem. Ser.* **1976**, *No. 154*. Robertson's data on low molecular weight PS show that $G_{IC}(\infty) \sim M$ and $K_{IC} \sim M^{1/2}$.
(15) Forbes, W. G.; McLeod, L. A. *Trans. IRI* **1958**, *30*(5), 154. Their data on fractionated samples of uncured natural rubber show that the green strength, $\sigma(\infty)$, behaves as $\sigma(\infty) \sim M^{1/2}$ and the tack stress at constant time, t_c, behaves as $\sigma \sim t_c^{1/4}M^{-1/4}$ for $M \leq 2.5 \times 10^6$.
(16) Wool, R. P. *Polym. Prepr., Am. Chem. Soc., Div. Polym. Chem.* **1982**, *23* (2), 62.